3D Printing by Multiphase Silicone/Water Capillary Inks

*Sangchul Roh, Dishit P. Parekh, Bhuvnesh Bharti, Simeon D. Stoyanov, and Orlin D. Velev**

3D printing of polymers is accomplished easily with thermoplastics as the extruded hot melt solidifies rapidly during the printing process. Printing with liquid polymer precursors is more challenging due to their longer curing times. One curable liquid polymer of specific interest is polydimethylsiloxane (PDMS). This study demonstrates a new efficient technique for 3D printing with PDMS by using a capillary suspension ink containing PDMS in the form of both precured microbeads and uncured liquid precursor, dispersed in water as continuous medium. The PDMS microbeads are held together in thixotropic granular paste by capillary attraction induced by the liquid precursor. These capillary suspensions possess high storage moduli and yield stresses that are needed for direct ink writing. They could be 3D printed and cured both in air and under water. The resulting PDMS structures are remarkably elastic, flexible, and extensible. As the ink is made of porous, biocompatible silicone that can be printed directly inside aqueous medium, it can be used in 3D printed biomedical products, or in applications such as direct printing of bioscaffolds on live tissue. This study demonstrates a number of examples using the high softness, elasticity, and resilience of these 3D printed structures.

The 3D printing technology has evolved impressively over the last decade in its ability to fabricate structures with complex topographical features on the micro and macroscale.[1–8] The 3D manufacturing via direct ink writing can shape various types of materials from plastics to metals by nozzle extrusion processes.[1,2,7,9–16] The inks for direct writing with polymers mostly contain thermoplastics, which allows hot melt nozzle extrusion followed by rapid cooling and solidification into target shape. It is more difficult to do 3D printing with elastomeric polymers, as their precursors are normally liquid at ambient conditions. The postejection curing complicates and slows down the process, which for some polymers can be speeded up by using special UV curing agents.[17]

One of the most widely used elastomeric polymers, polydimethylsiloxane (PDMS), has wide range of applications in the area of advanced materials for biomedical and soft robotics.[12,13,18–22] However, 3D printing with PDMS is challenging as it necessitates special compositions with UV-curable or thixotropic PDMS precursors.[3,19,21,22] Direct ink writing of non-flowable PDMS precursor has been used to fabricate synthetic spider web and micro chambers.[13,19,22] Wax microparticles have been incorporated in PDMS precursors to make gel-like materials forming stable structures after extrusion.[23] More recently, PDMS liquid precursors (LPs) were 3D printed by injection into hydrophilic thixotropic Carbopol gel, which acts as a scaffold/support.[24]

Capillarity can be a powerful alternative tool to shape "soft" 3D structures. Sandcastles formed by mixing sand with the right amount of water can be considered as the most ancient method of making 3D architectures. The structural stability of sandcastles is attributed to the formation of capillary bridges between the wetted sand granules.[25–32] Similar capillary bridges are found in concentrated multiphasic suspensions, containing small amount of immiscible liquid with <90° contact angle on the solid particles.[33–35] The interparticle capillary bridges lead to formation of 3D particle networks by pulling the adjacent particles together. These suspensions can have paste-like consistency and significant elastic modulus and static yield stress.[34,35] Such pastes behave as elastic, shape-retaining solids at low stress, and as viscoelastic flowable liquids at high stress. 3D assemblies of glass microbeads (MBs) linked via water capillary bridges by rapid water removal can retain their shape, albeit in fragile structures.[36] 3D printing with capillary bridged structures, however, requires multicomponent mixtures of solid suspension phase, surface-wetting liquid, and continuous medium. The need to simplify such systems begs the question: Can we create capillary suspension inks that use the same elastomeric material both as solid beads and as liquid phase for capillary bridging, which can later be transformed into one single elastomer compound?

We present here a new class of elastomeric 3D printing ink, which consists of three components: precured PDMS

S. Roh, D. P. Parekh, Prof. O. D. Velev
Department of Chemical and Biomolecular Engineering
North Carolina State University
Raleigh, NC 27695, USA
E-mail: odvelev@ncsu.edu

Prof. B. Bharti
Cain Department of Chemical Engineering
Louisiana State University
Baton Rouge, LA 70803, USA

Prof. S. D. Stoyanov
Physical Chemistry and Soft Matter
Wageningen University
Wageningen 6708 WE, The Netherlands

Prof. S. D. Stoyanov
Department of Mechanical Engineering
University College London
Torrington Place, London WC1E 7JE, UK

The ORCID identification number(s) for the author(s) of this article can be found under https://doi.org/10.1002/adma.201701554.

DOI: 10.1002/adma.201701554

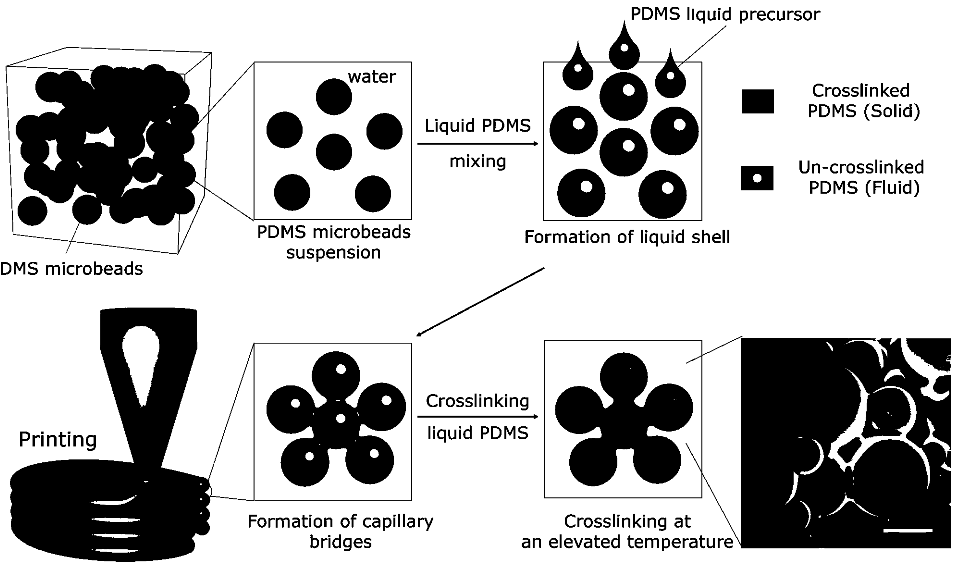

Figure 1. Principle of 3D printing process of PDMS particle suspension with capillary bridges. The PDMS microbead suspensions in water are mixed with liquid precursor. The suspensions turn into gels as LP forms capillary bridges among adjacent PDMS MBs. The gel-like suspensions are extruded into filaments via a nozzle. The 3D printed PDMS structures are heat-cured at 85 °C to crosslink the bridges and lock-in the structure from single silicone component (scale bar = 20 µm).

microbeads, uncured PDMS liquid precursor, and water medium. The liquid precursor binds the microbeads by capillarity, yielding a thixotropic extrudable gel-like phase. We characterize the mechanical properties of these capillary suspension gels. The gel phase can be arrested after extrusion by crosslinking (curing) of the liquid PDMS binding the microbeads, yielding 3D silicone structures that are highly elastic and stretchable. The capabilities of this approach are demonstrated by several unique objects fabricated by 3D printing in air and under water.

The conceptual schematic of the overall procedure for making these PDMS inks is described in **Figure 1**. First, a suspension of PDMS MBs is prepared by emulsification and thermal curing. We used Polysorbate 20 as a dispersion stabilizer during the PDMS bead synthesis. The suspension was then mixed with the PDMS LP using a mechanical mixer leading to surface wetting of the MBs with uncured LP. Direct surface contacts between the wetted MBs during the blending process lead to the formation of LP capillary bridges between the beads (Figure 1). The formation of these bridges transformed the free-flowing PDMS suspension into viscoelastic paste. The paste is extrudable and could be printed into 3D structures. These structures were further heat-cured at 85 °C to crosslink the liquid silicone bridges between the microbeads, resulting into robust, flexible, and elastic 3D architectures.

The mechanical stability of the extruded uncured 3D structures is strongly dependent on the viscoelastic characteristics of the PDMS ink. Such viscoelastic properties are commonly evaluated using dynamic oscillatory measurements.[11,18] We found that the addition of a small amount of liquid precursor into PDMS MB suspensions resulted in a large change in their rheological characteristics (with minimal effect on the bead size, Figure S1, Supporting Information). The dynamic moduli of the PDMS MB suspensions (50%, v/v) with and without 2 vol% of LP (2/98 = LP/MBs) were measured with small amplitude oscillatory shear measurement (**Figure 2**a). Without LP, the loss modulus (G'') is slightly higher than storage modulus (G'), and both G' and G'' show an angular frequency dependency indicating fluid-like behavior. With LP, the suspension becomes highly elastic and the dynamic moduli are nearly constant with frequency (Figure 2a,b). The formation of highly viscoelastic paste from MB suspension can be attributed to the formation of local interbead capillary bridges from the added LP. This is in agreement with previous reports on capillary bridged gels.[33–35,37] The presence of PDMS LP capillary bridges between the MBs was confirmed by fluorescence microscopy imaging (Figure 2b). The wetting and capillary bridging of the PDMS MBs with LP can be explained by the strong affinity between them arising from the similarity in their chemical composition (i.e., as both are siloxanes, the MBs are completely wetted by the LP).

The rheological characteristics of PDMS capillary suspension pastes were further measured with incremental addition of 10–40 vol% LP to the PDMS MBs. The data for G' versus the oscillatory shear stress of the suspensions are plotted in Figure 2c. All compositions of PDMS MBs and LP showed gel-like behavior at low shear stresses and yielding at high oscillatory shear stresses. The MB suspensions containing up to 20 vol% of LP showed both high yield stress and storage modulus (G'). However, yield stresses and storage moduli decrease as the amount of PDMS LP increased above 20 vol%, indicating the formation of weaker gels. This can be attributed to the morphological change of the suspension.[33,35,38–40] Up to 20 vol% of PDMS LP, capillary bridges were clearly observed in the scanning electron micrographs (Figure 2d and Figure S2, Supporting Information). As the concentration of PDMS LP increased, the MBs were saturated with LP as shown in Figure 2d. Even though the liquid bridges nearly disappeared at 30 vol% of LP, the suspension still had yield stress resulting from the liquid envelope around the beads that is able

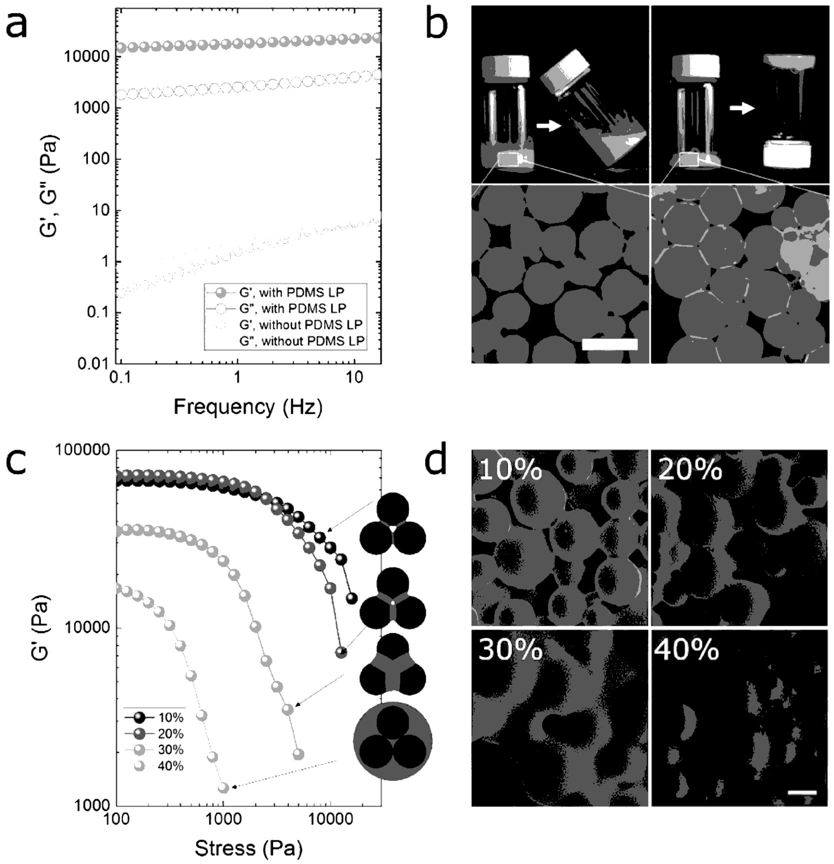

Figure 2. Characterization of capillary bridged PDMS microbead suspension. a) Change in the storage and loss modulus with the frequency of PDMS microbeads in water suspensions (50%, v/v) with/without 2 vol% of additional liquid PDMS precursor. b) Fluorescence imaging of PDMS suspension without (left) and with (right) 2 vol% of PDMS precursor. The PDMS MBs are tagged with Nile red (red), and LP phase contained Coumarin 6 (yellow). The micrographs show the structure of microbead ink where the added liquid precursor forms capillary bridges between the beads (scale bar = 20 µm). c) The elastic modulus of PDMS suspension mixed with various amounts of PDMS precursor plotted against the oscillation stress. d) Field emission scanning electron micrograph (FE-SEM) of suspensions with increasing amount of liquid precursor (scale bar = 20 µm). As the amount of surface wetting PDMS precursor increases (>20 vol%), the microbeads are engulfed in the matrix of liquid PDMS.

to induce negative capillary pressure.[38,41] However, when the added LP exceeded 40 vol%, the suspension effectively liquefied, behaving like a weak gel with a low yield stress and low elastic modulus. Therefore, the optimal liquid precursor composition in the suspension gel system was 2–30 vol%, yielding mechanically stable gels that are suitable as 3D printing inks.

Based on these data, we tested inks from PDMS suspension gels with 10%–30% liquid precursor. Notably, we could not use either PDMS suspension without LP or only liquid precursor as a 3D printing ink because these behave like fluids regardless of the presence of shear stress as shown in Figure S3 in the Supporting Information. However, inks containing liquid precursor were extrudable due to their liquid-like behavior ($G'' > G'$) at high shear stress but become solid-like material ($G' > G''$) again at low shear stress as shown in Figure S4 in the Supporting Information. The extruded microwires had stable 3D structures, indicating the presence of strong capillary attraction between the individual particles.[36,42] They formed uniform microfilaments after curing as shown in **Figure 3**a. The water phase in the ink formulation created cavities after it dried, leaving behind pores. The cross-sectional profile of the microfilament (with 20% LP) shows that the structure is uniformly porous throughout the fiber body (Figure 3a, bottom right). Figure 3b illustrates the fine structure of deposited fibers consisting of capillary bridged PDMS ink on a glass substrate through a nozzle of ID 100 µm. Considering that the average size of PDMS MBs is 10 µm, the fibers are composed of very small number of PDMS microbeads along the radial direction. At sub-millimeter length scale, an extruded liquid filament will deform due to Plateau-Rayleigh instabilities arising from its interfacial tension.[7,43] The lack of such instabilities in our thin PDMS fibers, implies that their structure is locked-in by the yield stress of the capillary bridged beads.

The extruded PDMS suspension "microfilaments" were thermally cured to yield elastic rubber-like materials. The liquid bridges between the microbeads in the inks were chemically crosslinked at 85 °C for 2 h. The thermal curing process leads to permanent physical binding of the MBs and immobilization of the extruded structure. This resulting cured PDMS structures were elastic and highly flexible. Tensile testing of the cured material was performed after molding them into "dog-bone" shapes. The tensile stress versus strain curves of such specimens are shown in Figure 3c. Notably, the samples bound with less than 10% of liquid precursor were fragile. Meanwhile, the PDMS specimens with >10% of PDMS binder were highly elastic, stretching to strains above 80% (Figure 3c). This result proves that the PDMS MBs can be reliably bound with PDMS bridges after crosslinking. As higher amounts of PDMS LPs were added, the tensile modulus and maximum elongation at break also increased. This increase in the tensile modulus of cured PDMS suspension with the increasing amount of PDMS binder is very different in functional dependence than the G' of uncured PDMS suspensions (Figure 2c). Smaller volume fractions of LP bind the suspension strongly, but result in a more porous cured material, which is detrimental for its tensile modulus.[44] These data suggest that the tensile module, elasticity, bendability, and stretchability of the printed structures can be conveniently controlled by the MB/LP ratio.

The applicability of these capillary suspension based inks was illustrated by shaping them using an extrusion 3D printing set-up (Figure S5, Supporting Information).[6] We made 3D structures via a direct ink writing type printing method with a syringe/needle microdeposition commonly used in bioprinting with viscoelastic inks.[12,22] The structure and the properties of the material that was extruded and cured are remarkable in several aspects. As illustrated above, these PDMS structures are highly extensible even though they are porous. The reason for the high tear resistance is that both the original beads and the postextrusion cured bridges are made of the same polymer, maximizing their cohesivity. They are also very elastic and bendable. As an example of the application of this macroscopic material elasticity, we printed a designed 3D metamaterial structure with the ink composed of PDMS MBs with 25% LP.[21,45] A macroscopic elastin-like structure printed and cured with the PDMS inks is shown in **Figure 4**a. The delicate highly stretchable structure readily conforms to various types of surfaces by changing its shape due to its ultraflexibility at various length scales.

Depending on the applied macroscopic stress, different topological features expand and stretch multifold, thus allowing creation of novel metamaterials with preprogramed, nonlinear response, and shape memory properties.[46–48] For instance, when these 3D printed PDMS mesh metastructures are brought in contact with water droplet, they can wrap around the surface of the droplet by forming a micrococoon similar to "capillary origami,"[49,50] as shown in Figure 4b and Movie S1 in the Supporting Information. This example illustrates that the surface capillary forces are comparable to the elastic forces into the 3D printed structures. Given that the later can be preprogramed by the 3D printed topological structure as well as by the properties of the "ink" (i.e., elastomer concertation and type, capillary suspension volume fraction, particle size, and even shape), this offers an unprecedented capability of designing new ultrasoft metamaterials.

The high elastic modulus and static yield stress of the PDMS capillary ink enable the extrusion of printed structures with excellent shape retention ability, which in turn facilitates rapid 3D printing in the *z*-direction. In Figure 4a, we illustrate the sculpting of a multilayered spiral structure consisting of PDMS MBs with 25% LP (dynamically shown in Movie S2 in the Supporting Information). It retained its as-printed shape with high precision. Another illustration of the 3D stability of deposited structures is presented in Figure 4d, where a 4.2 cm high tetrahedral frame composed of six filaments was extruded from a 410 µm diameter nozzle.

Owing to the biocompatibility and elasticity of silicone, its 3D printed objects can be essential for numerous biomedical applications.[12,22] Our PDMS capillary ink has the remarkable ability to be 3D printed directly in water, in biological media, and potentially even into live tissue. We simulated this environment by printing inside phosphate-buffered saline (PBS) solution and crosslinking the structures. Figure 4e and Movie S3 in the Supporting Information show a "cage" of PDMS ink (MB/LP = 7/3) printed in situ around an *N*-isopropylacrylamide (NIPAAm) hydrogel block (green color) immersed in a PBS solution. NIPAAm gel was chosen as the block substrate

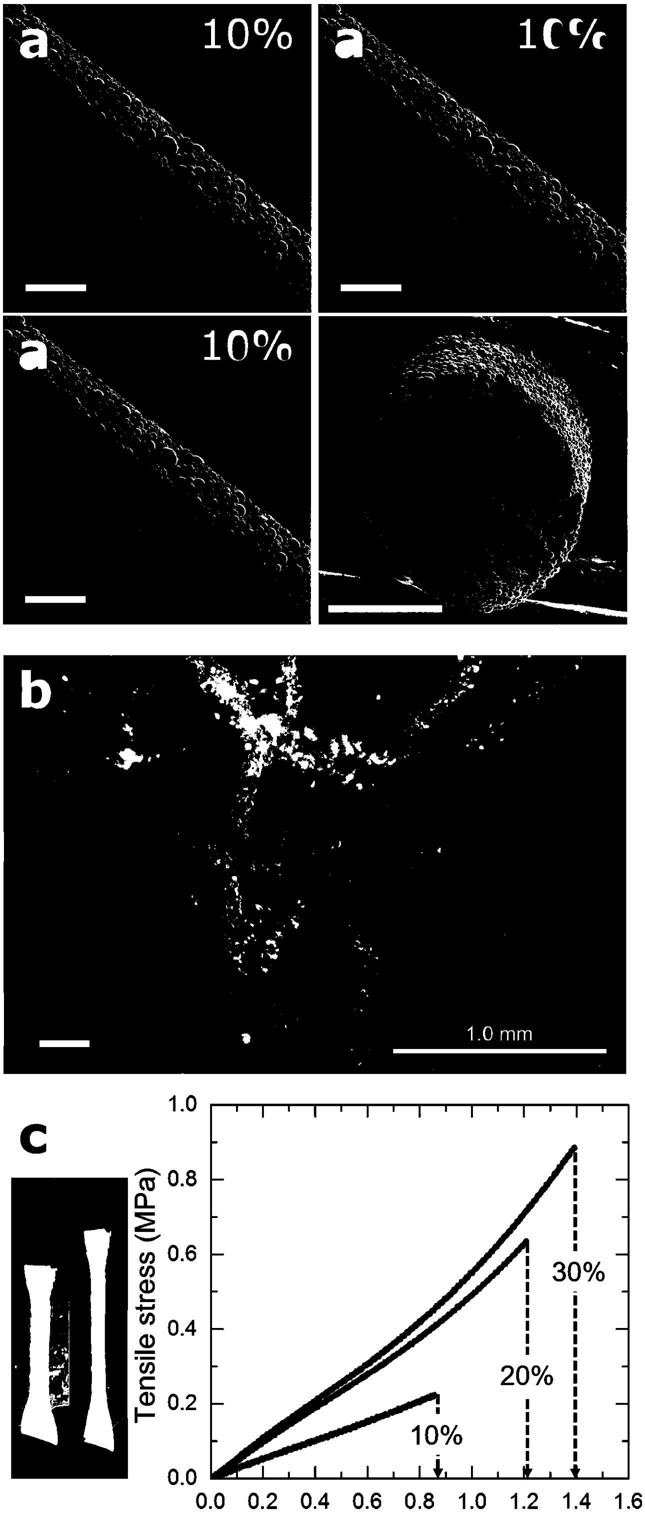

Figure 3. Morphologies and mechanical properties of crosslinked PDMS inks. a) FE-SEM images of PDMS inks with different LP volume fractions ejected through nozzle of inner diameter ≈410 µm (scale bar = 250 µm) and FE-SEM image of cross-section of printed PDMS wire with 20% liquid precursor (bottom right, scale bar = 250 µm). b) Optical and FE-SEM images of fine PDMS fibers formed from capillary suspension. The fibers preserve their shape even after ejection and crosslinking at 85 °C and their diameter illustrates the current resolution of the method (inset scale bar = 50 µm). c) A photograph of extension of a PDMS slab with 10% of liquid precursor and extensional tensile stress versus strain at increasing amount of initial LP precursor. The slope (Young's modulus) and maximum strain at break increase with larger amounts of the added precursor.

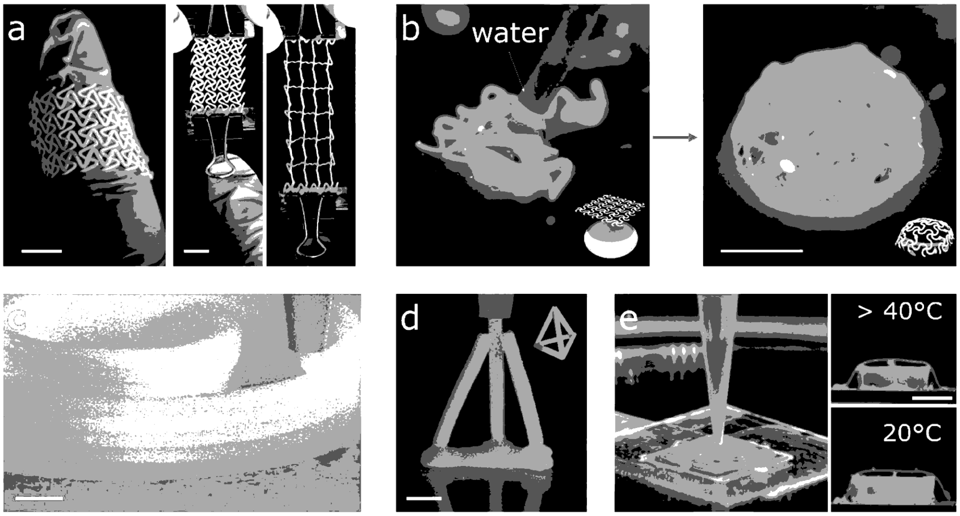

Figure 4. Examples of 3D printed ultraflexible PDMS structures made after curing of capillary-bridged bead suspensions. a) Elastin-like structure with high size extensivity and flexibility (scale bars = 10 and 5 mm, respectively). b) Wrapping and encapsulation of a single water droplet by an ultrasoft hydrophobic mesh (scale bar = 5.0 mm). c) Printing of multilayered spiral structure (scale bar = 1.0 mm). d) A snapshot of the process of printing of tetrahedral frame (scale bar = 1.0 mm). The ejected uncured structure is self-standing. e) PDMS ink printing under PBS solution around a NIPAAm hydrogel body (left). After crosslinking in water, the filaments of the printed "cage" could be highly stretched by temperature-triggered expansion of NIPAAm hydrogel body (right, top, and bottom, scale bar = 5.0 mm).

because it rapidly changes volume at its lower critical solution temperature (≈34 °C),[51,52] which further allows to test the elasticity of the printed cage. The NIPAAm hydrogel block was made by procedures reported previously.[52] We printed crossed cage filaments on the top of the NIPPAm hydrogel block, which were connected to a filaments frame printed on the underlying PDMS film (Figure 4e, left and Movie S3, Supporting Information). After crosslinking the printed filaments cage, we gradually decreased the temperature below the NIPAAm critical point. As the hydrogel block gradually expanded, the cage filaments stretched without breaking. This result points out that the capillarity based PDMS inks are printable and curable in situ under water, without loss of elasticity. Such printing can potentially be performed directly in contact with live tissue if light- or body-temperature triggered initiators are used.

In summary, we present a 3D printable multi-phase ink consisting of water and two silicone-based components. It contains crosslinked PDMS microbeads and liquid non-crosslinked PDMS phase. Owing to the capillary binding of the microbeads, suspensions containing certain fractions of PDMS liquid precursor behaved like pastes, which are flowable at high shear stress and possess high storage moduli and yield stresses that are needed for direct ink writing. These PDMS suspension pastes are directly extruded with air pressure and shaped on a 3D printer. Due to their mechanical stability, structures such as multilayered spirals and free-standing filaments could be printed. The liquid PDMS bridges were thermally crosslinked after printing. The crosslinked PDMS material exhibited excellent elasticity and stretchability. Its porosity and mechanical properties, such as tensile modulus, could be controlled by the fraction of liquid precursor in the original paste. Moreover, self-standing, elastic, and cohesive structures could be made by printing and curing the ink under aqueous solutions. As this ink is made of porous, biocompatible silicone it can be used in 3D printed biomedical products, or in applications such as direct printing of bioscaffolds on live tissue. The high softness, elasticity, and resilience of these 3D printed structures may also open new opportunities in soft robotics and stimuli-responsive materials.

Experimental Section

Synthesis of PDMS Microbeads: The synthesis of PDMS microbeads was performed in two steps: (1) emulsification of PDMS precursors (Sylgard 184, Dow corning) and (2) crosslinking of the emulsified PDMS precursor droplets. 10:1 mixtures of PDMS precursors and curing agents were mixed and degassed in a desiccator under vacuum. Aliquots of 6 mL of PDMS precursors were preemulsified in a 50 mL centrifuge tube containing 30 mL of 14 wt% polyvinyl alcohol (Mowiol 18-88, Sigma-Aldrich) aqueous solution on a vortex mixer (Vortex Genie 2, Scientific Industry, USA). The preemulsified PDMS emulsions were then further emulsified with a Servodyne electronic mixer (Cole-Parmer, Model # 50003, USA) at 3000 rpm. After emulsification, the PDMS emulsions were poured and stirred in deionized water at 85 °C for 2 h. The crosslinked PDMS microbeads were then rinsed ten times with 50 mL of aqueous solution of Polysorbate 20 (0.1 wt%, Sigma-Aldrich) for further use.

Preparation of PDMS Inks: As-prepared MBs in water suspension were thoroughly blended with liquid PDMS precursor (10/1 precursor/curing agent mixture). The postmixing step was facilitated by a vortex mixer and the suspension was further mixed with the Servodyne electronic mixer at 6000 rpm for 10 min. The resulting materials exhibited gel-like behaviors and were thoroughly blended using a mortar and pestle to obtain homogeneous mixtures. The multiphase dispersion has well-distributed PDMS liquid precursor forming uniform capillary bridges between the PDMS microbeads (Figure S6, Supporting Information). The final ink also contains ≈5%–40% water as an external run-off phase that makes possible the capillary binding and printing, but as the ratio between microbeads and water is not a system control parameter it was not varied further.

Characterization of PDMS Inks: For the rheological analysis of PDMS capillary suspensions, a plate-plate geometry (diameter: 25 mm) was used for both dynamic shear measurements with 1.0 mm gap size (AR 2000, TA instrument). Sand paper circles were attached to the plates to prevent wall slip. For the PDMS MB suspension without LP, a cone and plate geometry (diameter: 60 mm, 2°) was used. Every measurement was performed after oscillatory preshearing at 1 rad s^{-1} for 10 min with a strain of 0.5 and equilibrium for 10 min and 1.0 Hz for reproducible data. The small amplitude oscillatory measurement was conducted within the linear viscoelastic regime of the materials. The linear viscoelastic regime was determined via strain sweep test at fixed frequencies (1 and 100 rad s^{-1}). The tensile testing of the cured PDMS capillary suspensions was conducted after molding the suspensions into a dog-bone shape (ASTM D412). The crosshead speed of the testing was 5.0 mm min^{-1} (5943 Instron). Fluorescence microscopy (BX-61 microscope, Olympus) and field emission scanning electron microscopy (Verios 460L FE-SEM, FEI) were used to visualize and analyze the morphology of PDMS capillary suspensions and the deposited PDMS inks. Here the PDMS MBs were tagged in red color with Nile red dye (Sigma-Aldrich), and the capillary bridges were colored in yellow by addition of Coumarin 6 dye (Acros organics). After each marker component was mapped by fluorescence microscope, two color channels were merged through ImageJ software.

Supporting Information

Supporting Information is available from the Wiley Online Library or from the author.

Acknowledgements

This study was supported by funding from US National Science Foundation, CBET-1604116 and by the Research Triangle MRSEC on Programmable Soft Matter, DMR-1121107. The authors also thank NC State University for support through 2017 Chancellors Innovation Fund Award. The authors thank Drs. Michael Dickey and Saad Khan for generously providing the 3D printer, tensile testing machine, and rheometer.

Conflict of Interest

The authors declare no conflict of interest.

Keywords

3D printing, multiphase gel, soft matter, stimuli-responsive actuator

Received: March 19, 2017
Revised: April 17, 2017
Published online:

---

[1] G. M. Gratson, M. Xu, J. A. Lewis, *Nature* **2004**, *428*, 386.
[2] J. A. Lewis, *Adv. Funct. Mater.* **2006**, *16*, 2193.
[3] J. R. Tumbleston, D. Shirvanyants, N. Ermoshkin, R. Janusziewicz, A. R. Johnson, D. Kelly, K. Chen, R. Pinschmidt, J. P. Rolland, A. Ermoshkin, E. T. Samulski, J. M. DeSimone, *Science* **2015**, *347*, 1349.
[4] S. Hong, D. Sycks, H. F. Chan, S. Lin, G. P. Lopez, F. Guilak, K. W. Leong, X. Zhao, *Adv. Mater.* **2015**, *27*, 4035.
[5] C. B. Highley, C. B. Rodell, J. A. Burdick, *Adv. Mater.* **2015**, *27*, 5075.
[6] D. P. Parekh, C. Ladd, L. Panich, K. Moussa, M. D. Dickey, *Lab Chip* **2016**, *16*, 1812.
[7] C. Ladd, J.-H. So, J. Muth, M. D. Dickey, *Adv. Mater.* **2013**, *25*, 5081.
[8] J. J. Martin, B. E. Fiore, R. M. Erb, *Nat. Commun.* **2015**, *6*, 8641.
[9] J. A. Lewis, G. M. Gratson, *Mater. Today* **2004**, *7*, 32.
[10] S. L. Morissette, J. A. Lewis, P. G. Clem, J. Cesarano, D. B. Dimos, *J. Am. Ceram. Soc.* **2001**, *84*, 2462.
[11] Q. Li, J. A. Lewis, *Adv. Mater.* **2003**, *15*, 1639.
[12] D. B. Kolesky, R. L. Truby, A. S. Gladman, T. A. Busbee, K. A. Homan, J. A. Lewis, *Adv. Mater.* **2014**, *26*, 3124.
[13] M. Wehner, R. L. Truby, D. J. Fitzgerald, B. Mosadegh, G. M. Whitesides, J. A. Lewis, R. J. Wood, *Nature* **2016**, *536*, 451.
[14] A. S. Gladman, E. A. Matsumoto, R. G. Nuzzo, L. Mahadevan, J. A. Lewis, *Nat. Mater.* **2016**, *15*, 413.
[15] M. A. Skylar-Scott, S. Gunasekaran, J. A. Lewis, *Proc. Natl. Acad. Sci. USA* **2016**, *113*, 6137.
[16] M. R. Sommer, L. Alison, C. Minas, E. Tervoort, P. A. Rühs, A. R. Studart, *Soft Matter* **2017**, *13*, 1794.
[17] F. Zhou, W. Cao, B. Dong, T. Reissman, W. Zhang, C. Sun, *Adv. Opt. Mater.* **2016**, *4*, 1034.
[18] D. Kokkinis, M. Schaffner, A. R. Studart, *Nat. Commun.* **2015**, *6*, 8643.
[19] Z. Qin, B. G. Compton, J. A. Lewis, M. J. Buehler, *Nat. Commun.* **2015**, *6*, 7038.
[20] S. Shan, S. H. Kang, J. R. Raney, P. Wang, L. Fang, F. Candido, J. A. Lewis, K. Bertoldi, *Adv. Mater.* **2015**, *27*, 4296.
[21] A. Clausen, F. Wang, J. S. Jensen, O. Sigmund, J. A. Lewis, *Adv. Mater.* **2015**, *27*, 5523.
[22] D. B. Kolesky, K. A. Homan, M. A. Skylar-Scott, J. A. Lewis, *Proc. Natl. Acad. Sci. USA* **2016**, *113*, 3179.
[23] J. I. Lipton, S. Angle, H. Lipson, *2014 Annu. Int. Solid Freeform. Fabr. Symp.* **2014**, 848.
[24] T. J. Hinton, A. Hudson, K. Pusch, A. Lee, A. W. Feinberg, *ACS Biomater. Sci. Eng.* **2016**, *2*, 1781.
[25] M. Scheel, R. Seemann, M. Brinkmann, M. Di Michiel, A. Sheppard, B. Breidenbach, S. Herminghaus, *Nat. Mater.* **2008**, *7*, 189.
[26] A. Kudrolli, *Nat. Mater.* **2008**, *7*, 174.
[27] M. Pakpour, M. Habibi, P. Møller, D. Bonn, *Sci. Rep.* **2012**, *2*, 549.
[28] B. Bharti, A.-L. Fameau, M. Rubinstein, O. D. Velev, *Nat. Mater.* **2015**, *14*, 1104.
[29] P. A. Kralchevsky, K. Nagayama, *Adv. Colloid Interface Sci.* **2000**, *85*, 145.
[30] B. Bharti, A.-L. Fameau, O. D. Velev, *Faraday Discuss.* **2015**, *181*, 437.
[31] B. Bharti, D. Rutkowski, K. Han, A. U. Kumar, C. K. Hall, O. D. Velev, *J. Am. Chem. Soc.* **2016**, *138*, 14948.
[32] O. D. Velev, N. D. Denkov, V. N. Paunov, P. A. Kralchevsky, K. Nagayama, *Langmuir* **1993**, *9*, 3702.
[33] S. Van Kao, L. E. Nielsen, C. T. Hill, *J. Colloid Interface Sci.* **1975**, *53*, 367.
[34] H.-J. Butt, *Science* **2011**, *331*, 868.
[35] E. Koos, N. Willenbacher, *Science* **2011**, *331*, 897.
[36] J. Chopin, A. Kudrolli, *Soft Matter* **2015**, *11*, 659.
[37] J. N. Israelachvili, *Intermolecular and Surface Forces*, Academic Press, NY **1992**.
[38] S. M. Iveson, J. D. Litster, K. Hapgood, B. J. Ennis, *Powder Technol.* **2001**, *117*, 3.
[39] S. M. Iveson, J. D. Litster, *Powder Technol.* **1998**, *99*, 243.
[40] S. M. Iveson, J. D. Litster, *Powder Technol.* **1998**, *99*, 234.
[41] N. Mitarai, F. Nori, *Adv. Phys.* **2006**, *55*, 1.
[42] J. C. Conrad, S. R. Ferreira, J. Yoshikawa, R. F. Shepherd, B. Y. Ahn, J. A. Lewis, *Curr. Opin. Colloid Interface Sci.* **2011**, *16*, 71.
[43] L. Rayleigh, *Proc. R. Soc. London* **1879**, *29*, 71.
[44] J. Wang, *J. Mater. Sci.* **1984**, *19*, 801.

[45] K.-I. Jang, H. U. Chung, S. Xu, C. H. Lee, H. Luan, J. Jeong, H. Cheng, G.-T. Kim, S. Y. Han, J. W. Lee, J. Kim, M. Cho, F. Miao, Y. Yang, H. N. Jung, M. Flavin, H. Liu, G. W. Kong, K. J. Yu, S. Il Rhee, J. Chung, B. Kim, J. W. Kwak, M. H. Yun, J. Y. Kim, Y. M. Song, U. Paik, Y. Zhang, Y. Huang, J. A. Rogers, *Nat. Commun.* **2015**, *6*, 6566.

[46] J. B. Pendry, A. J. Holden, D. J. Robbins, W. J. Stewart, *IEEE Trans. Microwave Theory Tech.* **1999**, *47*, 2075.

[47] J. H. Lee, J. P. Singer, E. L. Thomas, *Adv. Mater.* **2012**, *24*, 4782.

[48] S. Babaee, J. Shim, J. C. Weaver, E. R. Chen, N. Patel, K. Bertoldi, *Adv. Mater.* **2013**, *25*, 5044.

[49] C. Py, P. Reverdy, L. Doppler, J. Bico, B. Roman, C. N. Baroud, *Phys. Rev. Lett.* **2007**, *98*, 156103.

[50] J. D. Paulsen, V. Démery, C. D. Santangelo, T. P. Russell, B. Davidovitch, N. Menon, *Nat. Mater.* **2015**, *14*, 1206.

[51] D. Morales, B. Bharti, M. D. Dickey, O. D. Velev, *Small* **2016**, *12*, 2283.

[52] D. Morales, I. Podolsky, R. W. Mailen, T. Shay, M. D. Dickey, O. D. Velev, *Micromachines* **2016**, *7*, 98.